CYCLIC STRESS-STRAIN BEHAVIOR OF REINFORCING STEEL INCLUDING EFFECT OF BUCKLING

By Mario E. Rodriguez,[1] Member, ASCE, Juan C. Botero,[2] and Jaime Villa[3]

ABSTRACT: It is expected that during strong earthquakes, longitudinal reinforcing steel in reinforced concrete structural elements may undergo large tension and compression strain reversals. Because of insufficient tie spacing, this repeated loading into the inelastic range may lead to buckling of steel reinforcing bars. Even though this problem has been studied by several researchers, most of these studies have been based on monotonic behavior. In this research, steel coupons were machined from steel reinforcing bars conforming to most of the ASTM A 706 specifications. These specimens were tested under axial-strain-controlled monotonic and reversed cyclic axial loading. The tests were performed until the specimens failed, in all cases under compressive loading. To study the effects of the ratio of spacing of lateral supports (S_h) to bar diameter (D) on reinforcement stability, tests were performed for S_h/D ratios of 2.5, 4, 6, and 8. Based on observed buckling behavior in reinforcing bars under cyclic (reversed) loading, a procedure is proposed for predicting onset of buckling. The use of this procedure, along with an analytical model proposed in the literature for the cyclic behavior of reinforcing steel, gave results that were in good agreement with experimental results obtained in this study.

INTRODUCTION

Results from moment-curvature analysis are important for evaluating the seismic performance of reinforced concrete (RC) elements. In this type of analysis, it is necessary to know the stress-strain behavior of reinforcing steel that includes the effect of buckling.

Even though the problem of reinforcement stability has been studied by several researchers, most of these studies have been based on a monotonic behavior, and limited research has been conducted considering the cyclic behavior of reinforcing bars including buckling (Monti and Nuti 1992; Mander et al. 1994; Suda et al. 1996; Pantazopoulou 1998). It is also worthy of mention that in most studies of reinforcement stability, a considerable scatter on the experimental load associated with buckling of reinforcing steel is expected for two reasons: (1) the variability of defining the buckling load based only on observation and (2) the difficulty in measuring strains in reinforcing bars in a concrete member after yielding. These factors have to be considered when evaluating existing data related to reinforcement stability or when conducting new research on the subject.

Several factors affect the onset of buckling of reinforcing bars in RC elements, such as the hoop influence on restraining a longitudinal bar, the splitting strength of cover concrete, or the lateral expansion of the concrete core at large compressive strains. The evaluation of the influence of these factors and their relationships is outside the scope of this investigation. This paper is aimed at studying the problem of reinforcement stability considering only the cyclic (reversed) behavior of reinforcing steel and the unsupported length of reinforcement. Results of an analytical and experimental investigation on reinforcement stability conducted at the National University of Mexico are described here. Based on these results, a procedure is proposed for evaluating the cyclic (reversed) stress-strain behavior of reinforcing steel including the effect of buckling.

MONOTONIC STRESS-STRAIN BEHAVIOR OF REINFORCING STEEL

Tension Monotonic Curve

A typical monotonic tensile stress-strain curve of reinforcing steel in tension is shown in Fig. 1. Mander et al. (1984) have proposed an idealization for the strain hardening that expresses a relationship between the stress f_s and the strain ε_s by

$$f_s = f_{su} + (f_y - f_{su}) \left(\frac{\varepsilon_{su} - \varepsilon_s}{\varepsilon_{su} - \varepsilon_{sh}} \right)^P \tag{1}$$

where f_y and f_{su} are the yield strength and ultimate strength, respectively; ε_{sh} and ε_{su} are the strain at which strain hardening commences and the ultimate strain, respectively. It must be noticed that the ultimate strain ε_{su} is defined here as the strain associated with the ultimate strength f_{su}. The parameter P is defined as

$$P = E_{sh} \left(\frac{\varepsilon_{su} - \varepsilon_{sh}}{f_{su} - f_y} \right) \tag{2}$$

where E_{sh} is the slope at the initiation of strain hardening. Instead of using E_{sh} for evaluating P, it is convenient to use an alternative definition of P:

$$P = \frac{\log \left(\frac{f_{su} - f_{sh1}}{f_{su} - f_y} \right)}{\log \left(\frac{\varepsilon_{su} - \varepsilon_{sh1}}{\varepsilon_{su} - \varepsilon_{sh}} \right)} \tag{3}$$

[1]Prof., Inst. of Engrg., Nat. Univ. of Mexico, Ap. Postal 70-290, Coyoacan, CP 04510, Mexico City, Mexico. E-mail: mrod@servidor.unam.mx

[2]Grad. Student, School of Engrg., Nat. Univ. of Mexico, Ap. Postal 70-472, Coyoacan, CP 04510, Mexico City, Mexico.

[3]Grad. Student, School of Engrg., Nat. Univ. of Mexico, Ap. Postal 70-472, Coyoacan, CP 04510, Mexico City, Mexico.

Note. Associate Editor: Walter H. Gerstle. Discussion open until November 1, 1999. To extend the closing date one month, a written request must be filed with the ASCE Manager of Journals. The manuscript for this paper was submitted for review and possible publication on October 15, 1998. This paper is part of the ***Journal of Structural Engineering***, Vol. 125, No. 6, June, 1999. ©ASCE, ISSN 0733-9445/99/0006-0605–0612/$8.00 + $.50 per page. Paper No. 19458.

where f_{sh1} and ε_{sh1} represent the ordinate and abscissa, respectively, of a selected point on the strain hardening curve.

Compression Monotonic Curve

Testing of reinforcing steel under compression has been less frequent than testing under tension. This is because of the ad- ditional difficulties in performing compression tests, mainly caused by potential buckling problems, inherent in this type of test. The lack of sufficient information on compressive test- ing of short reinforcing bars might explain why most studies on the seismic response of RC structures have been performed based on the assumption that a monotonic stress-strain curve of a short reinforcing bar in compression is equal and opposite

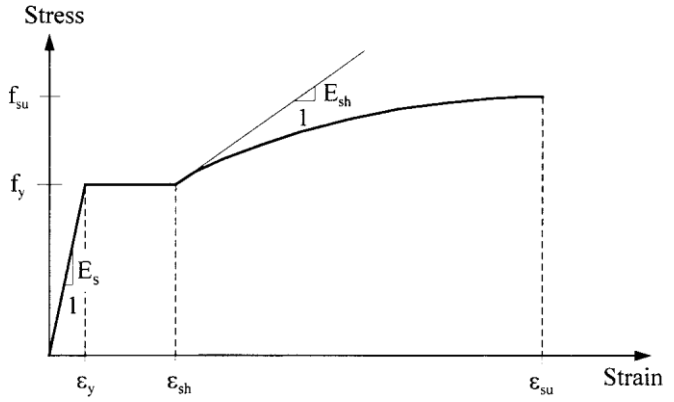

FIG. 1. Monotonic Stress-Strain Curve for Steel

to the corresponding curve in tension. However, experimental results have shown that when using the common definition of stress (which uses the initial cross-sectional area of the element), these curves are different (Mander et al. 1984; Dodd and Restrepo 1995). Dodd and Restrepo (1995) have found that in the natural coordinate system, which takes into account the instantaneous cross-sectional area of the element, the compression and tension curves are equal and opposite. Based on this finding, they defined the compressive stress, f_{cs}, and compressive strain, ε_{cs}, as follows:

$$f_{cs} = -f_s(1 + \varepsilon_s)^2 \tag{4}$$

$$\varepsilon_{cs} = \frac{-\varepsilon_s}{1 + \varepsilon_s} \tag{5}$$

Fig. 2 shows tension and compression stress-strain curves from monotonic tests on typical reinforcing steel (Rodriguez and Botero 1995) manufactured in Mexico. The ordinates in Fig. 2 represent nondimensional stresses, which were obtained by dividing the measured stresses by the corresponding yield stress of the specimens. This figure also shows the predicted compression curve, which was obtained using (4) and (5) and data measured in the tension tests. As seen in Fig. 2, the prediction of the compression stress-strain curve is in reasonable agreement with the measured curve. Dodd and Restrepo (1995) also found good agreement between a predicted compression curve using (4) and (5) and a measured compression curve obtained using data collected from tests on steel manufactured in New Zealand.

CYCLIC BEHAVIOR OF SHORT REINFORCING BARS

Several authors have proposed analytical models for estimating the cyclic stress-strain behavior of reinforcing bars in the absence of buckling (Mander et al. 1984; Dodd and Restrepo 1995). The model proposed by Dodd and Restrepo (1995) describes the Bauschinger effect by means of a softened curve and is based on data collected from reinforcing steel manufactured in New Zealand. This model uses the instantaneous geometry of the reinforcing bars. The model proposed by Mander et al. (1984) considers the Bauschinger effect and defines the cyclic stress-strain behavior using several rules for reversal from skeleton curves associated to the tension and compression cases. Fig. 3 shows results using this model and results of cyclic tests on Mexico manufactured reinforcing bars in the absence of buckling. A comparison of these curves shows a good agreement between the analytical and experimental results.

BUCKLING OF REINFORCING BARS

Several experimental and analytical investigations have been conducted in the past on buckling in reinforcing bars. However, most of these investigations have been performed considering monotonic loading and either the reduced or tangent modulus theory (Bresler and Gilbert 1961; Mander et al. 1984; Scribner 1986; Papia et al. 1988; Mau 1990; Watson et al. 1994). Limited research has been done on the stability of reinforcing bars under cyclic (reversed) loading. Monti and Nuti (1992) have proposed an analytical model for predicting the cyclic behavior of reinforcing bars including buckling. This model is based on results of a series of monotonic and cyclic tests on steel rebars and requires the calibration of several parameters using data from cyclic tests on reinforcing bars. Pantazopoulou (1998) has studied the mechanics of longitudinal bar buckling in RC elements and has shown the need to consider the interaction between tie effectiveness, tie spacing, core deformation capacity, and bar diameter. From an analysis of experimental evidence, this author has proposed design empirical rules for the tie spacing required to prevent buckling of longitudinal reinforcement. However, since the observed buckling strain was reported in only a few of the reviewed studies, the end of the member's usefulness was obtained from global response observations. That is, buckling strain was not considered directly.

Suda et al. (1996) have performed the only analytical and experimental study known of by the writers regarding the instability of reinforcing bars in RC elements under cyclic loading. They performed cyclic (reversed) loading tests on RC columns in which the reinforcing bars had a new instrumentation system for measuring strains beyond the yielding stage. Results of this research indicate that longitudinal bar buckling in RC elements subjected to cyclic (reversed) loading might occur when the bars are under a compressive stress in a tensile

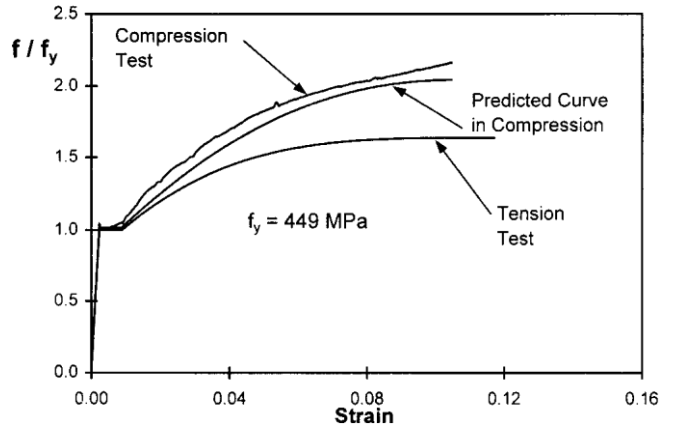

FIG. 2. Comparison of Tension and Compression Stress-Strain Curves

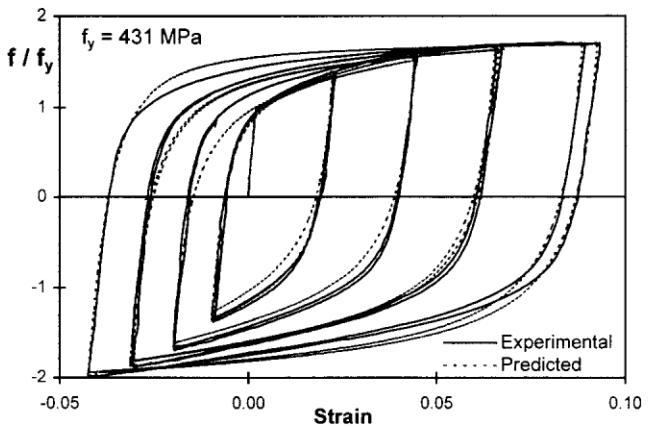

FIG. 3. Comparison of Predicted and Experimental Cyclic Stress-Strain in Absence of Buckling

strain range. Based on their findings, Suda et al. (1996) have proposed a model for representing the cyclic behavior of steel reinforcing bars in RC elements.

EXPERIMENTAL PROGRAM AND TESTING PROCEDURES

A series of monotonic and cyclic (reversed) tests of steel reinforcing bars were performed at the National University of Mexico for studying the instability of reinforcing bars. The steel reinforcing bars used in this series of tests were of reinforcing steel commercially available in Mexico and of the same type as that used in previous monotonic tests of steel rebars under tension (Rodriguez and Botero 1995). The stress-strain behavior of these steel rebars conforms to most of the ASTM A 706 specifications, which prescribe a minimum yield strength of 415 MPa and a minimum tensile strength of 550 MPa. Another control on tensile strength properties is that the tensile strength cannot be less than 1.25 times the actual yield strength.

Steel coupons of 16 mm diameter were machined from steel reinforcing bars of 31.8 mm diameter, complying with ASTM specifications (''Standard'' 1993). Fig. 4 shows typical geometry characteristics of the steel coupons tested in this research.

An important parameter in the stability of reinforcing bars in RC elements is the ratio of lateral support spacing, S_h, to bar diameter, D. In the test specimens, S_h is represented by the length of the specimen (Fig. 4). The S_h/D ratios selected for this study were 2.5, 4, 6, and 8, which can be considered representative of the tie spacing most commonly used in RC elements designed according to current building codes for seismic areas. The total tested numbers of specimens for the monotonic and cyclic tests were 10 and 26, respectively.

The tests were performed using an axial testing machine, model MTS-810. The specimens had both ends fixed to this testing machine as shown in Fig. 5. Also can be seen in Fig. 5, strains in the test specimens were measured using extensometers supported at opposite sides of the test specimens, with a constant gauge length of 30 mm (Fig. 4). The extensometers had enough resolution to evaluate the initiation of buckling, which, as discussed later, is defined using the differences between the readings from the strain gauges placed at both sides of the extensometer. The monotonic tests in compression had a target duration of about three minutes. The cyclic (reversed) tests, of a sinusoidal type with a constant frequency of 0.005 Hz, were displacement controlled, with two reversed cycles for each level of maximum axial strain. The target number for these levels of strains before buckling was 3.

Two cyclic strain histories considered for the cyclic tests were intended to represent cyclic strain histories to which longitudinal reinforcing bars of columns and beams might be subjected during an earthquake. In an RC column subjected to cyclic flexure, typically the neutral axis position is close to the middepth of the column section, which for increasing levels of lateral displacements leads to increasing straining in the tension and compression range. In an RC beam subjected to

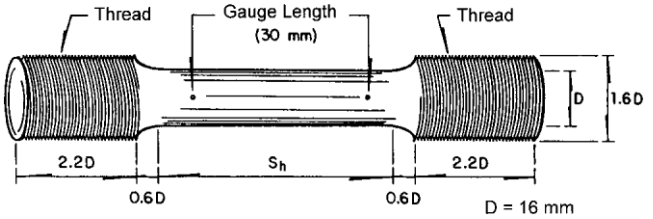

FIG. 4. Dimensions of Test Specimens

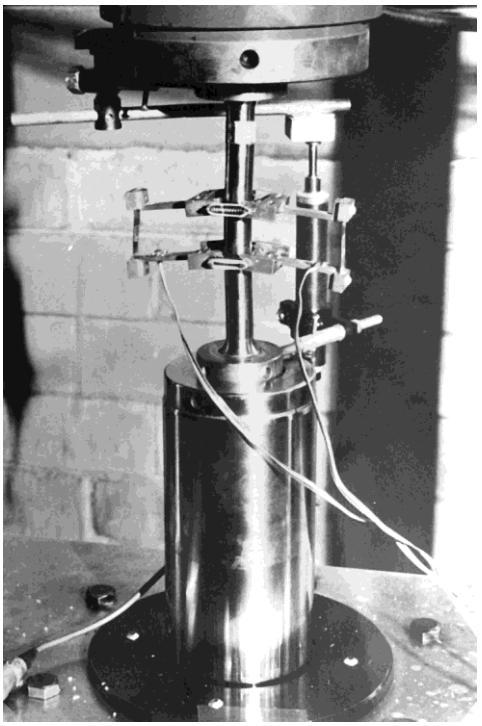

FIG. 5. View of Test Setup

cyclic flexure, typically the neutral axis is close to the extreme fiber in compression, with small strains for the steel in compression. Based on moment-curvature analyses of typical beam and column sections (Rodriguez 1999), typical values for the ratio $\varepsilon_m^+/\varepsilon_m^-$ were selected for this study, where ε_m^+ and ε_m^- are the maximum tensile and compressive strain for a longitudinal reinforcing bar in a strain cycle, respectively. For representing a seismic strain history in a column, the ratio $\varepsilon_m^+/\varepsilon_m^-$ was set equal to approximately 1 in eight specimens and to 2.3 in 13 specimens. A typical loading history for the latter type of testing is shown in Fig. 6. For a beam, the parameter ε_m^- was set equal to about 0; that is, the specimens for this case were subjected only to cycles in tension. This type of strain history was applied in five specimens.

A summary of specimens and their main characteristics for the monotonic and cyclic tests performed in this study is shown in Table 1. A complete documentation of the experimental data can be found elsewhere (Rodriguez and Botero 1998).

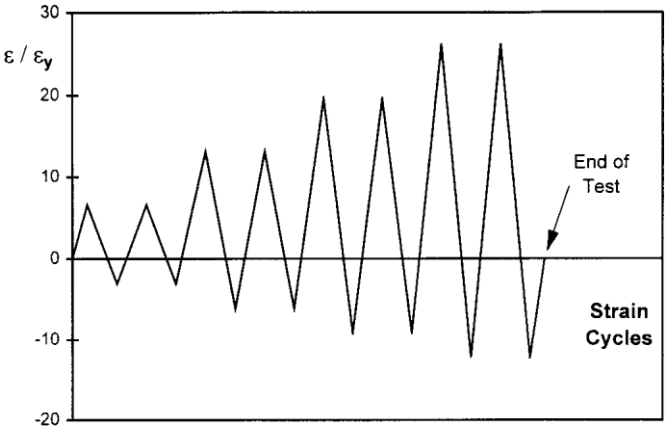

FIG. 6. Strain History Used for Cyclic Axial Loading Test of Specimens Representing a Reinforcing Bar of a Column (S_h/D = 4, E_m^+/E_m^- = 2.3)

MONOTONIC TESTS IN COMPRESSION

Definition of Onset of Buckling

Considerable variability for defining the onset of buckling in a reinforcing bar based only on observation is expected, since different observers of the same testing might indicate different initiations of buckling. To avoid this variability, in this research the definition of the onset of buckling was based on an experimental approach. This approach calls for using the strain readings at opposite faces of a specimen, namely ε_1 and ε_2, which were given by the extensometer previously described. The strain ε_1 is measured along with the fiber of the section that at buckling is subjected to an increase in compression (concave side), and the strain ε_2 is measured along with the fiber of the section subjected to a decrease in compression (convex side). According to the above discussion, the onset of buckling was defined when $\varepsilon_2 - \varepsilon_1$ was equal to or greater than 20% of ε_1.

Since it was not possible to know before testing the direction in which the specimen would buckle, the extensometers were not be placed in this direction. However, out of the total number of tested specimens, only two specimens buckled in a direction far from that in which the extensometers were placed.

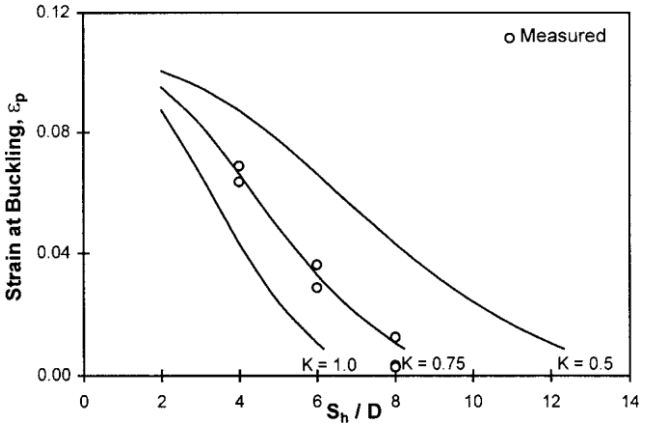

FIG. 8. Strain Data Fit to Model for Compressive Stress at Onset of Buckling in Monotonic Tests

Stress data shown in Fig. 7 can be compared there with predicted values using an analytical model for the compressive stress at the onset of buckling, f_p, based on the reduced modulus theory, which leads to

$$f_p = \frac{\pi^2 E_r}{16\left(K\frac{S_h}{D}\right)^2} \tag{6}$$

where E_r is the reduced modulus and K is the effective length factor. For calculating f_p with (6), a representative monotonic skeleton stress-strain curve of reinforcing steel in compression was defined using (4) and (5), which led to the following characteristic stress-strain control parameters: f_{yc} = -457 MPa; f_{suc} = -916 MPa; ε_{shc} = -0.0087; ε_{suc} = -0.1048; and P_c = 2.092. The subscript ''c'' here indicates that the parameters correspond to a monotonic compressive stress-strain curve, and the negative sign corresponds to a compressive stress or strain. Using the predicted value for f_p, the associated strain ε_p shown in Fig. 8 was evaluated from the selected monotonic skeleton stress-strain curve of a short reinforcing bar in compression.

Results using the above procedure for several values of the parameter K are shown in Figs. 7 and 8. It can be seen there that using a value of 0.75 for K leads to a good fit between results using the reduced modulus theory and the experimental data. This value of K suggests that the end conditions of the test specimens where between a pin-end and a fixed-end condition.

CYCLIC TESTS

Definition of the Onset of Buckling

The onset of buckling for the cyclic tests was defined by using the strain readings for ε_1 and ε_2 and relating these strains to the peak strains reached in the corresponding cycle, ε_m^+ and

set of Buckling in Monotonic Tests

FIG. 7. Stress Data Fit to Model for Compressive Stress at On-

ε^-. This critical condition was defined when $\varepsilon - \varepsilon$ was equal or greater than $0.2(\varepsilon^+ - \varepsilon^-)$. This approach for defining the onset of buckling in cyclic tests has the advantage that the definition given for a monotonic test is a particular case of the cyclic case. As seen later, the above definition of onset of buckling in a cyclic test will be used in a proposed procedure for predicting the strain associated with the buckling of a re- inforcing bar subjected to cyclic strain.

Fig. 9 presents the experimental cyclic stress-strain results in terms of the strains ε_1 and ε_2 for a specimen representing a reinforcing bar in a column with an S_h/D ratio equal to 6 and an $\varepsilon^+/\varepsilon^-$ ratio equal to 2.3. The black dot in Fig. 9 indicates the point of the stress-strain curve at the onset of buckling, obtained with the definition for the cyclic tests previously de- scribed. The results presented in Fig. 9 allow an evaluation of

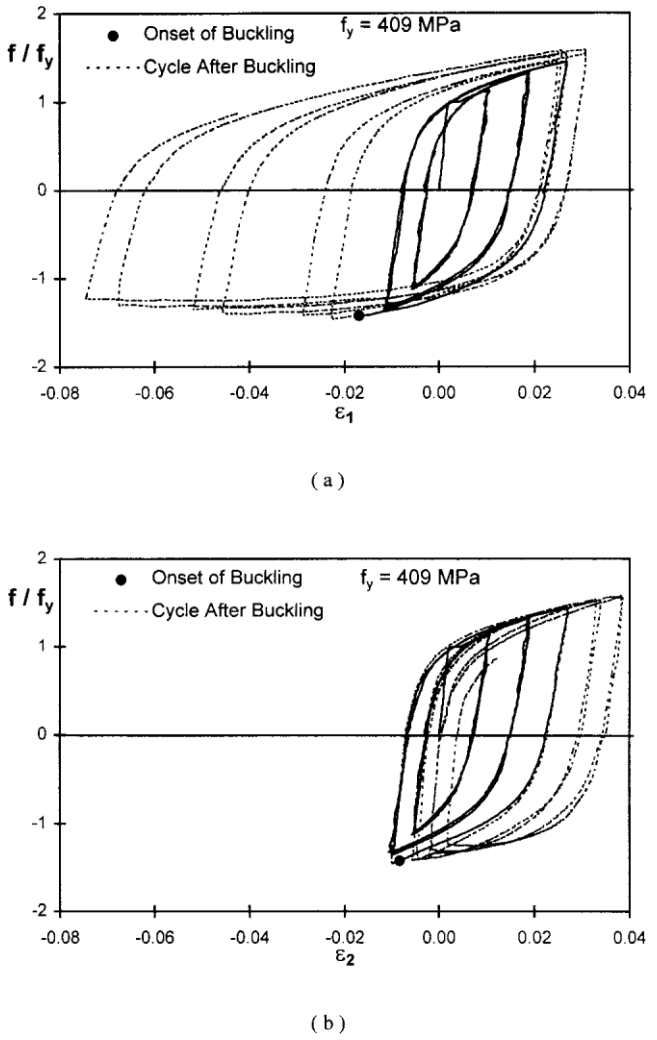

FIG. 9. Experimental Cyclic Stress-Strain Results for Specimen Representing a Reinforcing Bar in a Column (S_h/D = 6): (a) Concave Side; (b) Convex Side

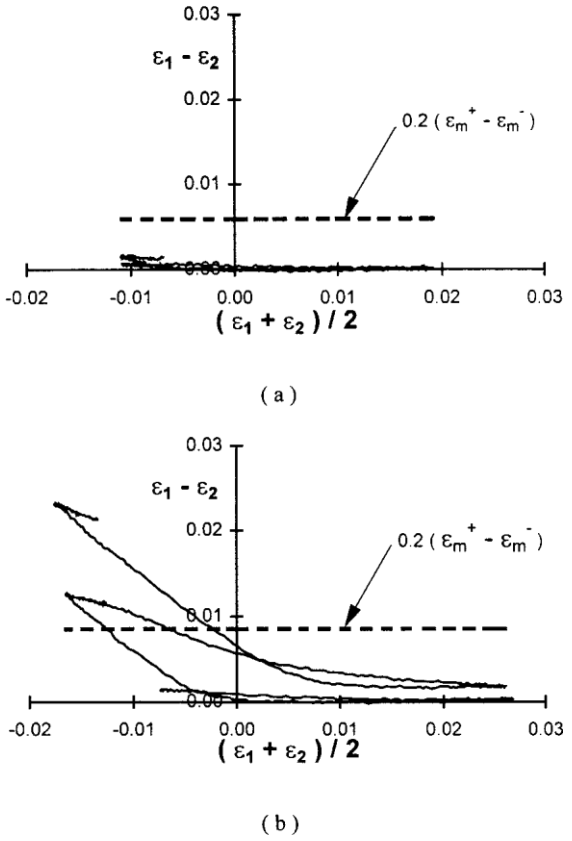

FIG. 10. Difference of Axial Strains Measured at Opposite Sides of a Specimen Representing a Reinforcing Bar in a Column (S_h/D = 6): (a) Level 2; (b) Level 3

the soundness of the proposed procedure for defining the onset of buckling. After this event (see stress-strain cycles after the black dots in Fig. 9) the difference in measured axial strains at both sides of the specimen becomes important. Furthermore, for increasing levels of the average axial strains in the specimens, the extreme fiber of the convex side of the specimen has increasing tensile strain incursions. Results of this type were also found for most of the specimens tested under cyclic loading (Rodriguez and Botero 1998).

Another form of illustrating the above discussed results is presented in Fig. 10, in which the measured difference $\varepsilon_1 - \varepsilon_2$ of the previously discussed specimen are showed there as a function of the average of ε_1 and ε_2. Results of Fig. 10 are presented for the two last levels of maximum cycle axial strains. As can be seen there, a sudden increase in the measured difference $\varepsilon_1 - \varepsilon_2$ occurs after the defined initiation of buckling, which supports the soundness of the proposed definition for the onset of buckling.

Proposed Procedure for Predicting Onset of Buckling

A procedure is proposed here for predicting the axial strain at onset of buckling of a reinforcing bar subjected to axial load reversals. This procedure uses the parameter ε_0^+, which is defined as the axial strain at zero loading after reversal from tension (Fig. 11). In addition, the parameter ε_p^*, which is used for evaluating the axial strain at buckling, ε_p, is defined as (Fig. 11)

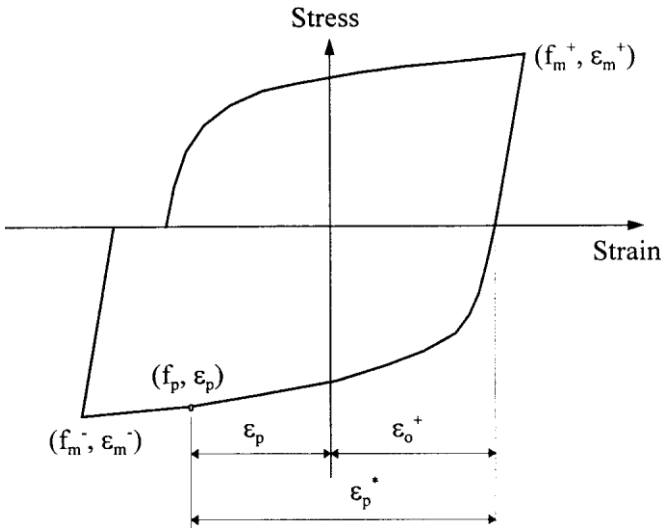

FIG. 11. Cyclic Stress Strain Curve for Steel

$$\varepsilon_p^* = \varepsilon_0^+ - \varepsilon_p \tag{7}$$

The above definition uses the hypothesis that the envelope for the compressive cyclic stress-strain curves reasonably coincides with the compressive monotonic curve. This hypothesis is based on results of monotonic and cyclic tests of reinforcing bars (Monti and Nuti 1992) and has also been used as a tool in analytical models for estimating the cyclic stress-strain behavior of reinforcing bars in the absence of buckling (Mander et al. 1984). An application of this hypothesis for the specimen previously discussed (S_h/D = 6, $\varepsilon_m^+/\varepsilon_m^-$ = 2.3) is illustrated in Fig. 12, which supports the validity of the mentioned hypothesis. The experimental results shown in Fig. 12 were obtained considering the measured axial loads and the corresponding

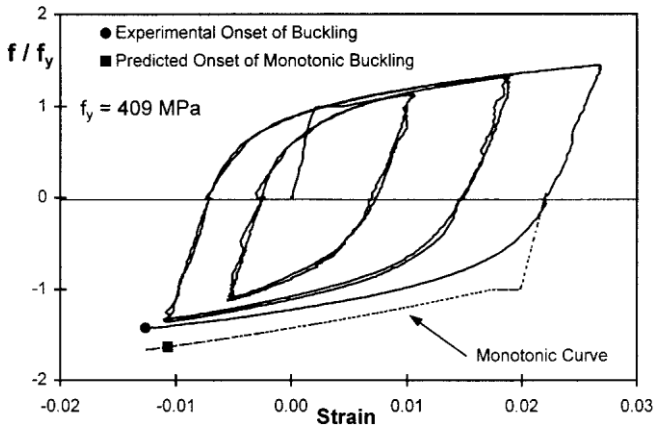

FIG. 12. Comparison of Cyclic and Monotonic Stress-Strain Curves for a Specimen Representing a Reinforcing Bar in a Column (S_h/D = 6)

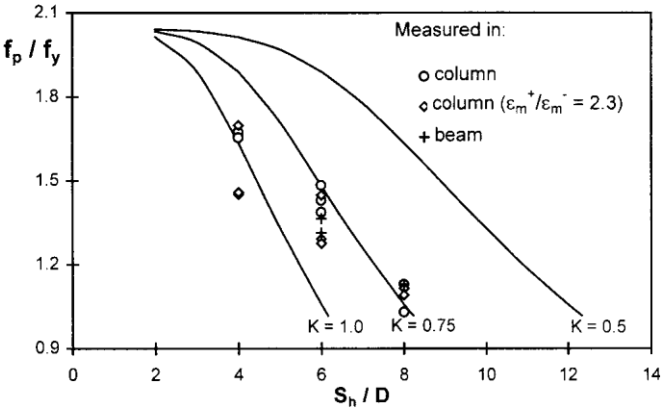

FIG. 14. Stress Data Fit to Model for Compressive Stress at Onset of Buckling in Cyclic Tests

average of ε_1 and ε_2. The same procedure for obtaining these experimental curves was also used in experimental cyclic stress-strain curves discussed below.

The measured values of ε_p^* for the specimens subjected to cyclic testing obtained with measured parameters ε_0 and ε_p and using (7) are shown in Fig. 13. Results for S_h/D ratios equal to 2.5 are not included in the figure, since specimens with this ratio did not show evidences of buckling. Results shown in Fig. 13 can also be compared there with predicted values for ε_p^*, that is, with the predicted monotonic strain at buckling considering 0.75 for K, and substituting this value for ε_p^*. These predicted values are shown in Fig. 13 by continuous curves corresponding to the 5% lower tail, average, and 95% upper tail values of the basic parameters that define the monotonic compression curve of the reinforcing steel used in this study. Measured axial loads at the onset of buckling, expressed in terms of non-dimensional stresses, f_p/f_y, are presented in Fig. 14, which also shows in continuous curves the predicted values for f_p/f_y that were obtained using the proposed predictive equations. The reinforcing steel properties considered in this evaluation were those corresponding to the average values previously mentioned.

It is worthy of mention that the predicted average curves for f_p and ε_p^* in Figs. 14 and 13 are the same as those shown in Figs. 7 and 8, respectively, with the variant that the parameter ε_p involved in the latter curves has been replaced by ε_p^* for obtaining the former curves.

Results shown in Fig. 14 indicate that the monotonic curve with K equal to 0.75 in most cases gives predicted values for f_p higher than the measured values, which indicates that the use of this procedure for evaluating reinforcing bar instability under hysteresis cycles might lead to unconservative results. A procedure for evaluating cyclic stress-strain curves of a reinforcing bar considering buckling is discussed later.

As for the measured and predicted values for ε_p^*, the results shown in Fig. 13 indicate that the average and 5% lower tail monotonic curves, with K equal to 0.75, in most cases are a lower bound for the measured ε_p^* values, which suggests that the proposed predictive equations can be used for obtaining a reasonable estimation of axial strain at the onset of buckling.

The above results indicate that the well-known reduced modulus theory for evaluating the strain in a reinforcing bar at the onset of monotonic buckling can also be used for evaluating the onset of buckling in a cyclic case, as long as the parameter ε_p^* is used instead of ε_p.

The experimental data found in this research indicate that the onset of buckling in a reinforcing bar under hysteresis cycles occurs after a reversal from tension and depends strongly on the maximum value of the tensile strain reached before that reversal. It is of interest that these results are similar to those obtained by Suda et al. (1996) in cyclic tests of RC elements, in the sense that buckling of a longitudinal reinforcing bar might occur in the tensile strain region of the cyclic stress-strain curve.

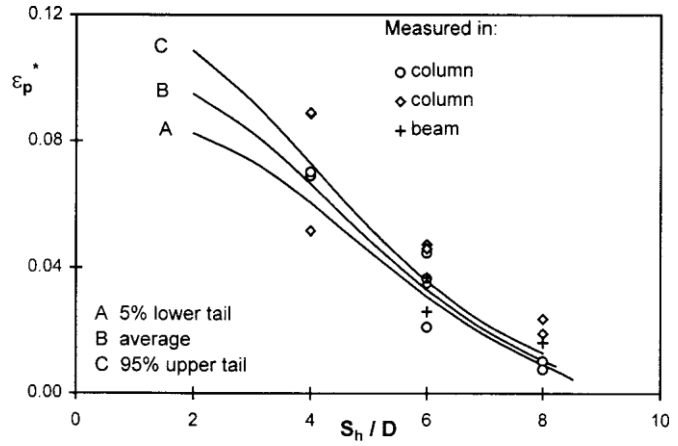

FIG. 13. Strain Data Fit to Model for Compressive Stress at Onset of Buckling in Cyclic Tests (K = 0.75)

Procedure for Evaluating Cyclic Stress-Strain Curves of Reinforcing Bar Considering Buckling

To evaluate cyclic stress-strain curves considering the onset of buckling, it is proposed to use the previously discussed analytical model of Mander et al. (1984) for estimating these curves in the absence of buckling. In this procedure, it is also proposed to use these curves until the predicted axial strain reaches the critical strain defined by the parameter ε_p^*.

Results of applying this procedure are shown in Fig. 15 for the same specimen whose results were presented in Figs. 9, 10, and 12 (S_h/D = 6, $\varepsilon_m^+/\varepsilon_m^-$ = 2.3). From the comparison between experimental and analytical stress-strain curves shown in Fig. 15, it can be seen that the proposed procedure fits the experimental data quite well. Similar results were found for other values of S_h/D and $\varepsilon_m^+/\varepsilon_m^-$ (Rodriguez and Botero 1998).

It must be mentioned that the proposed procedure neglects the additional axial deformation capacity of a reinforcing bar after the defined onset of buckling. However, in this stage, this deformation capacity is associated with an important reduction in axial stiffness (Monti and Nuti 1992; Mander et al. 1994), and the stiffness of the bar after buckling is mainly flexural (Monti and Nuti 1992).

It is also worthy of mention that the specimens tested in this research do not closely represent those other factors that

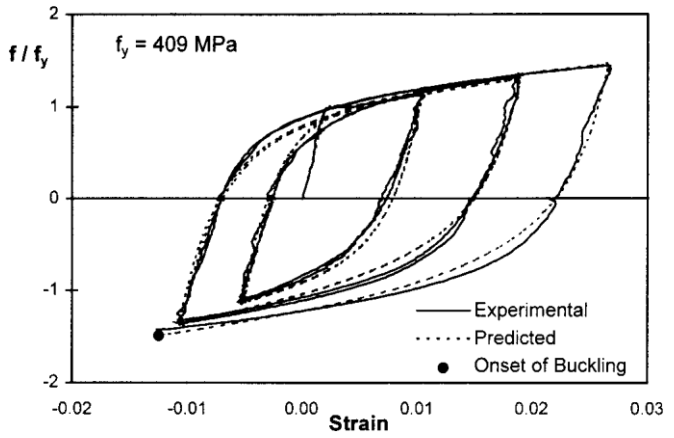

FIG. 15. Comparison between Predicted and Experimental Cyclic Stress-Strain Curves for a Specimen Representing a Reinforcing Bar in a Column ($S_h/D = 6$)

affect the onset of buckling of reinforcing bars in RC elements, as mentioned earlier. However, a more elaborate model of the onset of buckling in a reinforcing bar in an RC element should consider not only these factors but also the important influence on this failure mode of the proposed parameter ε_p^*.

Example Application of Use of Proposed Procedure for Modeling Compressive Steel Behavior

In order to discuss the potential behavior of a typical RC element subjected to cyclic load if a more accurate model was used for the compressive steel behavior, an example application is presented in the following.

For the sake of simplicity, only the cyclic (reversed) behavior of reinforcing steel and the unsupported length of reinforcement are considered in the example. Several other factors that affect the onset of buckling of reinforcing bars in RC elements are neglected.

Typical details for the beam section chosen for this example are shown in Fig. 16(a). Theoretical moment-curvature analyses were performed for this section. The idealized cyclic stress-strain curves for reinforcing steel used in these analyses were obtained following a conventional procedure and the one proposed for modeling the compressive steel behavior. In the conventional procedure, the compressive stress at the onset of buckling, f_p, is evaluated using (6). As for the tensile steel behavior, it is assumed that the section deformation capacity is reached when the steel strain in tension is equal to ε_{su}. The tension and compression skeleton curves involved in the idealized cyclic stress-strain curves for reinforcing steel were those previously used for predicted values shown in Figs. 7 and 8. The stress-strain curve for confined concrete proposed by Park et al. (1982) was used in the analyses, and the fracture of transverse reinforcement was defined according to the model proposed by Scott et al. (1982). The compressive cylinder strength, f'_c, was taken equal to 29 MPa. The unsupported length of reinforcement was evaluated assuming a value of 0.5 for the effective length factor, K (Watson et al. 1994).

Following the procedure discussed above, Fig. 16(b) shows theoretical moment-curvature relations derived for the beam investigated. The solid lines in this figure represent the hysteresis loops obtained when the compressive steel behavior is modeled with the proposed procedure, that is, using the parameter ε_p^*. The dashed line in Fig. 16(b) represents the additional hysteresis loops that are obtained if the compressive steel is modeled with the conventional procedure. These results show that the maximum available curvature is overestimated by 65% when considering the conventional procedure. As seen in Fig. 16(b), with the conventional procedure the

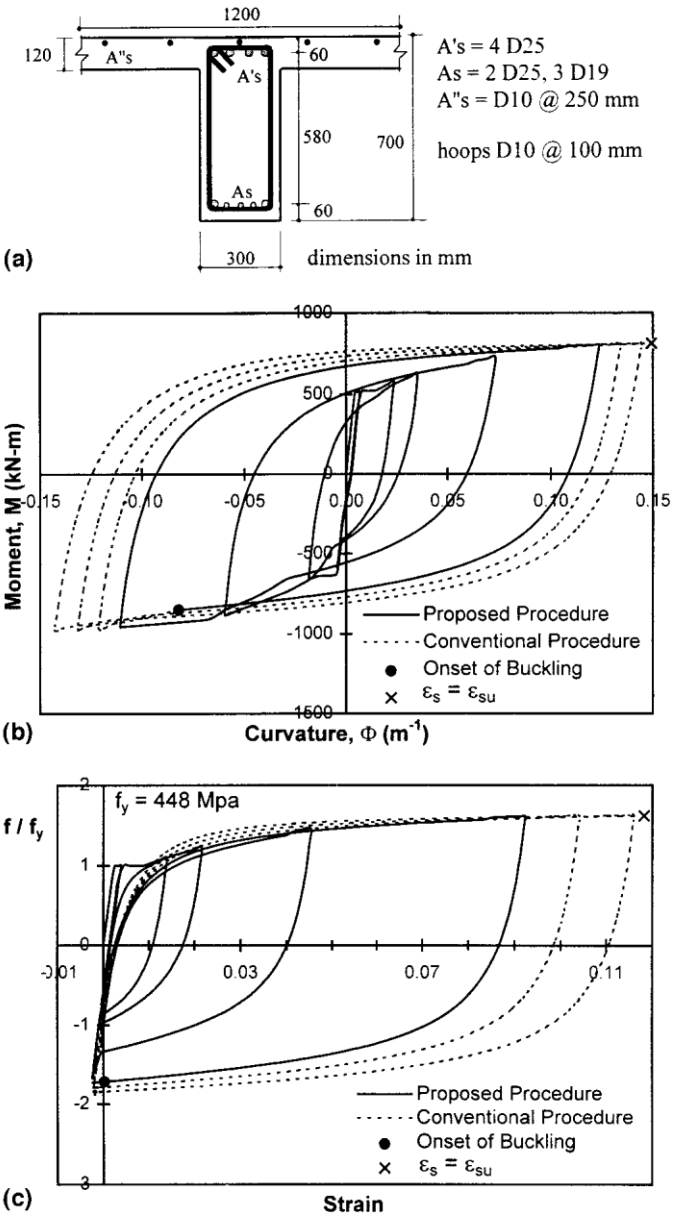

FIG. 16. Example Application for a Beam Subjected to Cyclic Load: (a) Section Investigated; (b) Moment-Curvature Curves for Critical Section; (c) Stress-Strain Relations for Bottom Longitudinal Reinforcement

critical condition in the beam section is reached when the bottom reinforcement reaches the tensile strain ε_{su}; with the proposed procedure the critical condition is governed by buckling of the reinforcement itself. Fig. 16(c) shows stress-strain relations for the bottom reinforcement of the beam under study, which allows a better understanding of the tensile and compressive behavior of this reinforcement. According to these results, the conventional procedure might lead to a significant overestimation of the tensile and compressive steel deformation capacity compared with the results using the proposed procedure.

CONCLUSIONS

Based on monotonic and cyclic (reversed) axial tests on steel rebars conducted at the National University of Mexico, a procedure is proposed for evaluating the cyclic (reversed) stress-strain behavior of steel rebars including the effects of buckling. It is shown here that the onset of buckling in a steel rebar subjected to hysteresis cycles might occur after a reversal

from tension and that it depends strongly on the maximum value of the tensile strain reached before that reversal. In this case, the onset of buckling of a steel rebar might occur in the tensile region of the hysteresis cycle.

Although the specimens tested in this research do not closely represent several factors affecting the onset of buckling in reinforcing bars in RC elements subjected to earthquakes, the proposed procedure for evaluating the onset of buckling in a steel rebar captures an important factor of reinforcing bar instability under hysteresis cycles.

ACKNOWLEDGMENTS

The writers gratefully acknowledge the financial support provided for this study by the Departamento del Distrito Federal (Mexico City) and the Instituto de Ingenieria (UNAM). Thanks are due to G. Monti of the Universita ''La Sapienza'' di Roma, Italy, and to the anonymous reviewers for their critical reading of the manuscript. Thanks are also given to J. Restrepo from the University of Canterbury, New Zealand, for his assistance in designing the extensometer used in this investigation.

APPENDIX. REFERENCES

Bresler, B., and Gilbert, P. H. (1961). ''Tie requirements for reinforced concrete columns.'' *ACI J.*, 58(26), 555–569.

Dodd, L. L., and Restrepo-Posada, J. I. (1995). ''Model for predicting cyclic behavior of reinforcing steel.'' *J. Struct. Engrg.*, ASCE, 121(3), 433–445.

Mander, J. B., Priestley, M. J. N., and Park, R. (1984). ''Seismic design of bridge piers.'' *Rep. 84-2*, Dept. of Civ. Engrg., University of Canterbury, Christchurch, New Zealand.

Mander, J. B., Panthaki, F. D., and Kasalanati, A. (1993). ''Low-cycle fatigue behavior of reinforcing steel.'' *J. Mat. in Civ. Engrg.*, ASCE, 6(4), 453–468.

Mau, S. T. (1990). ''Effect of tie spacing on inelastic buckling of reinforcing bars.'' *ACI Struct. J.*, 87(6).

Monti, G., and Nuti, C. (1992). ''Nonlinear cyclic behavior of reinforcing bars including buckling.'' *J. Struct. Engrg.*, ASCE, 118(12), 3268–3284.

Pantazopoulou, S. J. (1998). ''Detailing for reinforcement stability in RC members.'' *J. Struct. Engrg.*, ASCE, 124(6), 623–632.

Papia, M., Russo, G., and Zingone, G. (1988). ''Instability of longitudinal bars in RC columns.'' *J. Struct. Engrg.*, ASCE, 114(2), 445–461.

Park, R., Priestley, M. J. N., and Gill, W. (1982). ''Ductility of squared-confined concrete columns.'' *J. Struct. Div.*, ASCE, 8(4), 929–950.

Rodriguez, M. (1999). ''Effects of cyclic behavior of reinforcing steel on seismic performance of reinforced concrete members.'' *Developments of seismic steel reinforcements products and systems*. American Concrete Institute, Farmington Hills, Mich., in press.

Rodriguez, M., and Botero, J. C. (1995). ''Seismic behavior of structures considering mechanical properties of Mexico manufactured reinforcing steel.'' *Revista de Ingenieria Sismica*, 49, 39–50 (in Spanish).

Rodriguez, M., and Botero, J. C. (1998). ''Behavior of reinforcing bars subjected to monotonic and cyclic axial loading including buckling.'' *Rep. No. 610*, Instituto de Ingenieria, National University of Mexico, Mexico City, Mexico (in Spanish).

Scott, B. D., Park, R., and Priestley, M. J. N. (1982). ''Stress strain behavior of concrete confined by overlapping hops and high strain rates.'' *ACI J.*, 79(1), 13–27.

Scribner, C. (1986). ''Reinforcement buckling in reinforced concrete flexural members.'' *ACI J.*, 83, 966–973.

''Standard test methods for tension testing of metallic materials.'' (1993). *ASTM EM 8M-93*, ASTM, West Conshohoken, Pa.

Suda, K., Murayama, Y., Ichinomiya, T., and Shimbo, H. (1996). ''Buckling behavior of longitudinal reinforcing bars in concrete column subjected to reverse lateral loading.'' *Proc., 11th World Conf. on Earthquake Engrg.*, Elsevier Science, New York, Amsterdam.

Watson, S., Zahn, F., and Park, R. (1994). ''Confining reinforcement for concrete columns.'' *J. Struct. Engrg.*, ASCE, 120(6), 1798–1824.